

- ⁴⁵E. L. Berger, *Phys. Rev.* **179**, 1567 (1969).
⁴⁶M. J. Longo *et al.*, *Phys. Letters* **36B**, 560 (1971).
⁴⁷G. Ascoli *et al.*, *Phys. Rev. Letters* **25**, 962 (1970).
⁴⁸J. Ballam *et al.*, *Phys. Rev. Letters* **21**, 934 (1968).
⁴⁹J. T. Carroll *et al.*, *Phys. Rev. Letters* **25**, 1393 (1970).

- ⁵⁰G. Ascoli *et al.*, *Phys. Rev. Letters* **26**, 929 (1971);
 J. V. Beaupre *et al.*, *Phys. Letters* **34B**, 160 (1971).
⁵¹R. Silver, Caltech Ph.D. thesis, 1971 (unpublished).
⁵²M. Aderholz *et al.*, *Nucl. Phys.* **B8**, 45 (1968).
⁵³W. C. Harrison *et al.*, *Phys. Rev. Letters* **28**, 775 (1972).

Rapidity and Angular Distributions of Charged Secondaries According to the Hydrodynamical Model of Particle Production*

P. Carruthers[†] and Minh Duong-van

Laboratory of Nuclear Studies, Cornell University, Ithaca, New York 14850

(Received 1 March 1973)

Recent measurements of inclusive production cross sections are analyzed in the framework of the Landau hydrodynamical model of particle production. We also give a critical analysis of recent data and the variables used in their presentation. It is concluded that the evidence for a flat rapidity distribution in the central region is not compelling. Except possibly at the very highest available ISR (CERN Intersecting Storage Rings) energy, the Landau Gaussian gives an excellent description of the rapidity distribution of the nonleading charged secondaries. The calculation of distributions in the variable $\eta = -\ln \tan(\theta/2)$ from given rapidity and transverse momentum distributions is worked out in many interesting cases. The Landau rapidity distribution is cast in a universal (energy dependent) scaling law which agrees well with available data. The angle and energy dependence of charged secondaries near 90° in the c.m. system in pp collisions agrees well with the theoretical prediction. Finally it is shown that the hydrodynamical model leads to approximate Feynman scaling except for very small values of $x = 2p_{\parallel}/\sqrt{s}$, where large deviations from scaling are predicted.

I. INTRODUCTION

The description of particle production in high-energy collisions has recently attracted a great deal of attention. Experiments at the CERN intersecting storage rings (ISR) and NAL are beginning to reveal interesting patterns in such processes. The approximate validity of scaling laws has been established for inclusive cross sections and is perhaps the most striking single result. No adequate theory yet exists which gives a satisfactory description of the data. We refer¹⁻³ to some recent review articles which summarize experimental results and the partial insights obtained from various phenomenological models.

The main purpose of the present paper is to resurrect Landau's hydrodynamical model⁴ of particle production and particularly to elaborate its phenomenological consequences pertinent to recent experimental work. Secondly, we discuss some purely phenomenological questions having to do with the rapidity variable and the related "cosmic-ray" variable $\eta = -\ln \tan(\theta/2)$ (Secs. II and III). The hydrodynamical model, which was well regarded in the 1950's, suggests a number of interesting lines of research when cast in modern garb. Here we

shall analyze the experimental consequences of the most simple version of the model, in an extension of previous work by the authors.⁵ This version involves rather brutal approximations to the complicated equations of the complete theory and hence could give a distorted picture of the theory's true predictions.

The hydrodynamical model can be regarded as an extension of Fermi's statistical model.⁶ One envisions a thin slab of hot hadronic matter in thermal equilibrium just after the collision; strictly speaking this is a "head-on" collision picture, but one can imagine that a fraction of the collision products are described by this initial condition while leading particles carry away a sizeable fraction (of the order of $\frac{1}{2}$) of the energy and perhaps most of the angular momentum.¹ In Landau's model the particles do not jump right out into phase space (which leads to too many heavy particles in Fermi's picture), but undergo an expansion phase before breaking up. The force responsible for the expansion is large in the longitudinal direction (the pressure gradient is mainly in the longitudinal direction because of the Lorentz contraction) and provides a natural dynamics for the well-known transverse-longitudinal asymmetry

of secondary momenta. In addition, the predominance of pions is claimed to be a consequence of the cooling of the medium during expansion.

The detailed calculations are made on the basis of the classical relativistic hydrodynamics of a perfect fluid, whose energy momentum tensor $T^{\mu\nu}$ is

$$T^{\mu\nu} = (\epsilon + p)u^\mu u^\nu - g^{\mu\nu} p, \quad (1.1)$$

where $u^\mu(x)$ is the four-velocity field and ϵ, p are the scalar densities of energy and pressure. The hydrodynamic equations are simply

$$\partial^\mu T_{\mu\nu} = 0. \quad (1.2)$$

In order to solve these equations one needs in addition an equation of state, taken by Landau to be

$$p = \frac{1}{3}\epsilon, \quad (1.3)$$

which is characteristic of blackbody radiation. It is not surprising that (1.3) is equivalent to the vanishing of the trace of $T^\mu{}_\nu$

$$T^\mu{}_\mu = \epsilon - 3p. \quad (1.4)$$

Thus the expansion phase is treated by a scale-invariant dynamics; the scale of length enters through the initial condition (the ratio of the thickness and radius of the Lorentz-contracted proton is $\gamma = E/m_p$ in the c.m. frame) and the temperature characteristic of the system at the moment of breakup ($T \approx m_\pi = 140$ MeV). [The effect of changing the equation of state has been studied^{7,8}; however, we shall use (1.3) in this paper.] A brief supplementary bibliography of works extending or justifying Landau's approach is given in Refs. 9–16.

A second feature of Landau's approach is the assumption of adiabaticity in the expansion process. [This is actually implied by the form of Eq. (1.1).] A straightforward consequence is the multiplicity formula $N = KE^{1/4}$, where E is the laboratory proton energy. When E is measured in GeV, the constant K (not predicted by the theory) is found to be about 2.0. This power law, which has been used for years in cosmic-ray work, gives at least as good a fit¹⁷ to the data as the currently fashionable logarithmic form expected in multiperipheral models.

A decided virtue of the point of view of the model is its independence of the actual hadronic coordinates which best describe the highly excited hadronic matter. A second feature of the thermodynamic approach is that the precise nature of the interactions and even equations of motion are unimportant provided that the requisite local thermodynamic equilibrium is maintained. The details of the final stage, in which the fluid breaks up into asymptotic states of the system, remain

quite obscure, as in the parton model. We remark that the parton model should provide the simplest context in which to study the approximation of the full quantum-mechanical problem by the quasiclassical perfect fluid. The general problem of isolating those interactions which tend to establish local equilibrium (for which the averaged fields of thermodynamics, $\epsilon(x), p(x)$, etc., are the correct hadronic variables) from the interactions causing scattering in the usual sense is a deep and interesting problem which has scarcely been studied in hadron physics. Some preliminary efforts in this direction will be found in Refs. 13–16. We plan to outline an approach to this problem elsewhere.

In the present paper we shall discuss the gross properties of inclusive reactions. Most of the applications will be to $p\bar{p}$ collisions, since the theory is simple (symmetry in the c.m. frame) and since all available ISR and NAL data are of this type. More sensitive tests of the model, such as correlations, charge dependence of cross sections, etc., are left to subsequent work.

Our procedure relies on the work of Milekhin,⁹ who showed that the essential content of the three-dimensional solution to Landau's model was that the transverse motion is statistical (described by a Bose distribution in the local rest frame of the fluid at the moment of breakup) and that the longitudinal distribution is given by Landau's Gaussian falloff in p_\perp can be regarded as an approximation to his formulas. Cooper and Schonberg¹⁸ have recently obtained excellent numerical agreement with inclusive data using a (corrected) version of Milekhin's analysis. Here we shall use the simpler exponential (and also Gaussian) transverse distributions. The reader is invited to regard these as purely phenomenological formulas if he so chooses.

Sections II and III are devoted to a number of kinematical facts which are essential for a meaningful comparison with experiment. We investigate the shape of distributions in the experimentally convenient variable $\eta = -\ln \tan(\theta/2)$ for flat and Gaussian rapidity distributions. The difference between these variables is quite significant, as pointed out by Lyon, Risk, and Tow¹⁹ but sometimes ignored by subsequent workers. Section IV is in part a polemic against premature or misleading conclusions based on confusion of the rapidity with the variable η . Detailed analysis of the available experimental information shows that there is little convincing evidence for the long-awaited (multiperipheral) plateau in the rapidity distribution except possibly at the very highest accessible ISR energy ($\sqrt{s} = 53$). The remaining data are

surprisingly well described by Landau's energy-dependent Gaussian rapidity distribution [see Eq. (2.1) for the definition of y]

$$\frac{1}{\sigma_{\text{in}}} \frac{d\sigma}{dy} = \frac{dN}{dy} = N \exp(-y^2/2L)/(2\pi L)^{1/2}, \quad (1.5)$$

where the parameter L is

$$L = \frac{1}{2} \ln(s/4m_p^2), \quad (1.6)$$

where s is the squared total c.m. energy.

It must be kept in mind that the form (1.5) and the width formula (1.6) are but crude mathematical approximations to the full content of the model (which is in turn perhaps a crude approximation to the physical situation). Nevertheless the clarity of expression allowed by these oversimplified formulas is to be preferred in a preliminary investigation such as this one.

The apparent success of (1.5) (which involves no arbitrary parameters once the multiplicity is fixed at a single energy) over almost the entire range of available energy of 30 GeV and greater could mean that multiperipheral asymptopia is either wrong or essentially out of reach with contemporary apparatus.

In Sec. V evidence from other reactions (γp , πp , Kp) is scrutinized and found to support (1.5), provided that the Gaussian is not centered at zero. In Sec. VI, Eq. (1.5) is rewritten in a universal form involving the variable $z = y/\sqrt{L}$ and the distributions dN/dz shown to be in agreement with current experimental information. Section VII discusses the angle and energy dependence of the inclusive differential cross section near 90° in the c.m. system, according to the Landau picture. Finally, in Sec. VIII it is shown that our version of Landau's model gives approximate Feynman scaling²⁰ for $x = 2p_{\parallel}/\sqrt{s}$ not too small. For very small x substantial deviations occur. From our point of view the variable x has no natural role in the theory.

II. KINEMATICAL PRELIMINARIES

From the point of view of relativistic invariance the most useful coordinates describing an emitted particle are the transverse momentum p_{\perp} and the rapidity y :

$$y = \frac{1}{2} \ln \frac{E + p_{\parallel}}{E - p_{\parallel}}. \quad (2.1)$$

Under Lorentz transformations along the p_{\parallel} axis rapidity transforms additively:

$$y_2 = y_1 + y_{12}, \quad (2.2)$$

where $y_{12} = \ln[\gamma(1 + \beta)]$ depends on the usual β, γ

values relating coordinate frames 1 and 2. In much of the present paper we shall be concerned with "integrated" distributions dN/dy or $dN/d\Omega$ rather than the full double-differential cross sections. For instance, the number distribution

$$\frac{dN}{dy} = \frac{1}{\sigma_{\text{in}}} \frac{d\sigma}{dy}$$

is obtained by integrating the single-particle inclusive distribution

$$E \frac{d^3\sigma}{dp^3} = f(p_{\perp}, y, s) \quad (2.3)$$

over the transverse momentum p_{\perp} and dividing by the inelastic cross section σ_{in} . Throughout we shall have in mind the inclusive reaction $pp \rightarrow \pi + \text{anything}$, unless otherwise stated. This special case accounts for the bulk of produced particles in pp collisions. In many experimental situations it is much simpler to measure angles than to separately determine p_{\perp} and p_{\parallel} . The variable analogous to (2.1) in this case is

$$\eta = -\ln \tan(\theta/2). \quad (2.4)$$

It is useful to rewrite this in the form

$$\eta = \frac{1}{2} \ln \frac{p + p_{\parallel}}{p - p_{\parallel}}. \quad (2.5)$$

The variables η and y appear to be almost equivalent. It has already been noted that, because of the bounded transverse momentum distribution, particles in the central region are sufficiently nonrelativistic that the η distribution is substantially depressed relative to the rapidity distribution.^{5,19} We find that these distributions also differ at large angles, a fact which is not so obvious although required by equality of areas of the integrated distributions.

In order to derive $dN/d\eta$ from (2.1) we have to integrate over p for fixed η . The volume element d^3p is

$$d^3p = p^2 \text{sech}^2 \eta dp d\eta d\phi, \quad (2.6)$$

which is to be compared with

$$\frac{d^3p}{E} = p_{\perp} dp_{\perp} dy d\phi \quad (2.7)$$

used for the pair of variables \vec{p}_{\perp}, y . Some useful relations among the variables are

$$\begin{aligned} \tanh y &= p_{\parallel}/E, \\ \tanh \eta &= p_{\parallel}/p, \\ \text{sech} \eta &= p_{\perp}/p, \\ y &= \tanh^{-1}(v \tanh \eta), \end{aligned} \quad (2.8)$$

where $v = p/E$. The last two of Eqs. (2.8) allow us

to express the right-hand side of Eq. (2.1) as a function of p and η . The "priority" of the variables is not just a theoretical bias but can be motivated by the simplicity of data plotted in terms of p_{\perp} and y .

Since the bulk of the produced particles are pions, we shall work out this case in detail. The cross section $d\sigma/d\eta$ is

$$\frac{d\sigma}{d\eta} = 2\pi \operatorname{sech}^2 \eta \int_0^{\infty} \frac{p^2 f(p \operatorname{sech} \eta, y(p, \eta), s) dp}{(p^2 + m_{\pi}^2)^{1/2}}, \quad (2.9)$$

which is to be contrasted with

$$\frac{d\sigma}{dy} = 2\pi \int_0^{\infty} p_{\perp} f(p_{\perp}, y, s) dp_{\perp}. \quad (2.10)$$

(The true upper limit is determined by phase space. In almost every case we consider, the integrand cuts off sufficiently rapidly that this effect can be ignored.) It has already been noted^{5,19} that, at 90° in the c.m. frame, $d\sigma/d\eta$ and $d\sigma/dy$ differ by the average transverse pion velocity

$$\left(\frac{d\sigma}{d\eta}\right)_{\eta=0} = \langle v \rangle \left(\frac{d\sigma}{dy}\right)_{y=0}. \quad (2.11)$$

This result follows directly from Eqs. (2.9) and (2.10); the average is taken with the distribution

$$\frac{pf(p, 0, s)}{\int dp pf(p, 0, s)}.$$

There are two popular forms for fitting the p_{\perp} dependence of the data, namely exponential and Gaussian:

$$f_1(p_{\perp}) = B_1^2 e^{-B_1 p_{\perp}}, \quad (2.12)$$

$$f_2(p_{\perp}) = 2B_2^2 e^{-B_2^2 p_{\perp}^2}. \quad (2.13)$$

We have normalized these distributions in a uniform way so that

$$\int_0^{\infty} p_{\perp} f_i(p_{\perp}) dp_{\perp} = 1. \quad (2.14)$$

The corresponding values of $\langle v \rangle$ are given by

$$\langle v \rangle_1 = \int_0^{\infty} \frac{\xi^2 e^{-\xi}}{(\xi^2 + \mu_1^2)^{1/2}} d\xi \quad (2.15)$$

and

$$\langle v \rangle_2 = 2 \int_0^{\infty} \frac{\xi^2 e^{-\xi^2}}{(\xi^2 + \mu_2^2)^{1/2}} d\xi, \quad (2.16)$$

where the parameters μ_i are given by

$$\begin{aligned} \mu_1 &= mB_1, \\ \mu_2 &= mB_2. \end{aligned} \quad (2.17)$$

Since $\langle v \rangle$ does not depend on the particle mass separately from the slope parameter B , it is easy to convert from one particle type to another, using Table I. Preferred²¹⁻²³ values of B_1 and B_2 for pions appropriate to NAL and ISR experiments are $B_1 \approx 6$ (GeV/c)⁻¹ and $B_2^2 \approx 10$ (GeV/c)⁻². In our computations we shall use $B_1 m_{\pi} = 0.875$. It will be noted that for pions $d\sigma/d\eta$ differs from $d\sigma/dy$ by about 20% near 90° in the c.m. frame. For a given slope the effect is even bigger for heavier particles, such as K mesons (see Fig. 5 and the accompanying discussion). In the following section we give more extensive and detailed examples.

III. ANALYSIS OF $\ln \tan(\theta/2)$ DISTRIBUTIONS IN TERMS OF RAPIDITY DISTRIBUTIONS

In the absence of complete double differential cross-section measurements one needs theoretical input to compute $d\sigma/d\eta$ from $d\sigma/dy$. At present this essentially means that one either makes informed guesses based on earlier experiments or employs semitheoretical formulas. In this paper we adopt (2.12) or (2.13) as a factor of the full distribution and assume that

$$f = f_i(p_{\perp}) g(y, s). \quad (3.1)$$

Of course, the slope constant B_i may have a slight energy dependence. Detailed analysis at conventional (20–30 GeV) energies^{24,25} suggests that one may need a sum of, say, two terms of this form for a good fit to the data. Our purpose here is to exhibit the main effects without becoming bogged down in the mass of detail required to obtain great accuracy.

Actually, the functional form of (3.1) is the leading approximation to Milekhin's version of the hy-

TABLE I. The average emitted pion velocity at 90° in the c.m. frame is shown for transverse momentum distributions of the form $f_1 \propto \exp(-B_1 p_{\perp})$ and $f_2 \propto \exp(-B_2^2 p_{\perp}^2)$. The favored experimental values for moderate p_{\perp} values are $B_1 \approx 6$ GeV⁻¹ and $B_2^2 \approx 10$ GeV⁻².

B_1 (GeV ⁻¹)	1	2	3	4	5	6	7	8	9	10
$\langle v \rangle_1$	0.986	0.953	0.920	0.885	0.852	0.819	0.788	0.758	0.730	0.704
B_2^2 (GeV ⁻²)	1	2	3	4	5	6	8	9	12	16
$\langle v \rangle_2$	0.964	0.938	0.918	0.900	0.884	0.870	0.845	0.833	0.803	0.770

drodynamical model, in which the transverse distribution is dominated by thermal motion rather than hydrodynamic flow. It is very interesting that the hydrodynamic picture leads to approximate factorization in y and p_{\perp} . Whether the corrections will lead to agreement with facts when computed in the model remains to be seen.

Most of our attention will be directed towards two choices of the rapidity distribution g :

$$g_M(y, s) = \text{const.}, \quad (3.2)$$

$$g_L(y, s) = \frac{\exp(-y^2/2L)}{(2\pi L)^{1/2}}. \quad (3.3)$$

We have labeled these functions by M and L because the corresponding g 's are characteristic predictions of the multiperipheral^{26,27} and Landau⁴ models, respectively. The Landau model gives a specific prediction for L , but one can simply regard (3.3) as a smooth parametrization of various data. (These questions form the subject of Sec. IV.)

a. Flat rapidity distribution. The multiperipheral model and the parton model naturally lead to the prediction of a flat rapidity distribution in the "central region" at sufficiently high energy. Lyon,

Risk, and Tow have shown¹⁹ that a flat distribution in y leads to a dip in the η distribution. They used a p_{\perp} distribution of the form (2.13). We verify their result and, in addition, show that the exponential gives similar (stronger) effects. For the exponential case we find the ratio

$$R_1(\eta) = \frac{d\sigma}{d\eta} / \frac{d\sigma}{dy} = \int_0^{\infty} \frac{\xi^2 e^{-\xi} d\xi}{(\xi^2 + \mu_1^2)^{1/2}}, \quad (3.4)$$

$$\mu_1 = mB_1 \text{sech } \eta.$$

(Note that $d\sigma/dy$ is constant.) Figure 1 shows the dependence of $R_1(\eta)$ on η for pions ($m_{\pi} B = 0.875$); for various values of B_1 the dip does not heal until η reaches a value of about 2.

In the case of a Gaussian p_{\perp} distribution (2.13) the required ratio is (Fig. 2)

$$R_2(\eta) = \frac{d\sigma}{d\eta} / \frac{d\sigma}{dy} = 2 \int_0^{\infty} \frac{\xi^2 e^{-\xi^2} d\xi}{(\xi^2 + \mu_2^2)^{1/2}}, \quad (3.5)$$

$$\mu_2 = mB_2 \text{sech } \eta.$$

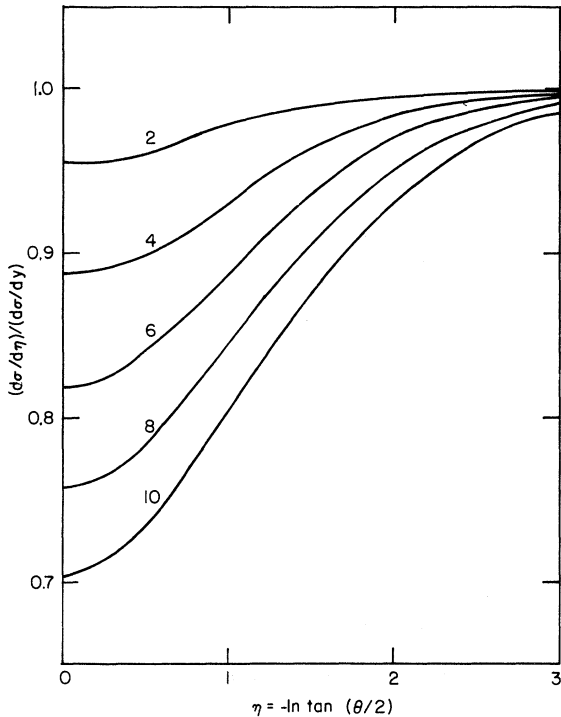


FIG. 1. The ratio $R_1 = (d\sigma/d\eta)/(d\sigma/dy)$ for pion production is illustrated for a flat rapidity distribution and an exponential transverse distribution of the form $\exp(-B_1 p_{\perp})$, for several values of B (B in GeV^{-1}). (The experimentally preferred value is about 6.25 for pions.)

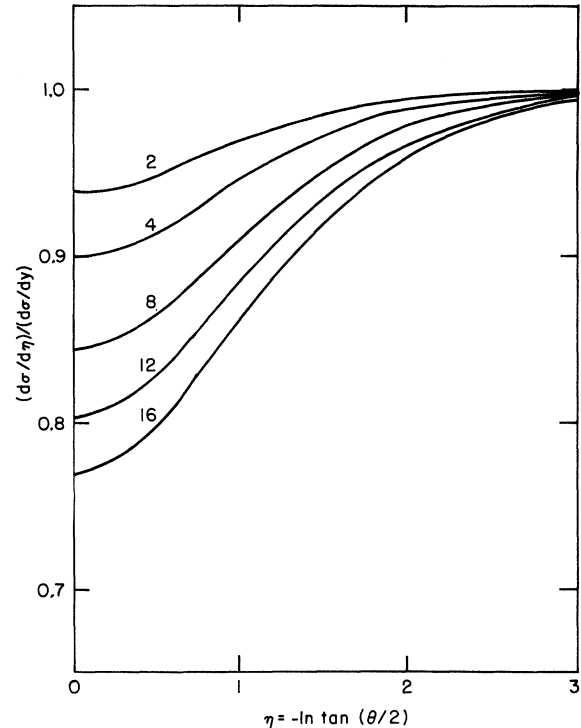


FIG. 2. The ratio $R_2(\eta) = (d\sigma/d\eta)/(d\sigma/dy)$ for pion production is illustrated for a flat rapidity distribution and a Gaussian transverse distribution of the form $\exp(-B_2^2 p_{\perp}^2)$ for several values of B_2^2 . (The experimentally preferred value of B_2^2 is 10–12 for pions.)

b. Gaussian rapidity distribution. It is clear from the foregoing calculation that a flat η distribution corresponds to a peaked rapidity distribution. Since it is easier to go from y to η than vice versa we use (3.3) to compute $d\sigma/d\eta$. We find that at sufficiently high energy the Gaussian in y becomes flattened in η in the range $-1 \lesssim \eta \lesssim 1$. Consider the normalized distribution

$$f_1(p_\perp, y, s) = \frac{N\sigma_{in} B_1^2}{(2\pi)^{3/2} L^{1/2}} \exp(-B_1 p_\perp - y^2/2L), \quad (3.6)$$

where N is the multiplicity, and use Eq. (2.9) to predict $d\sigma/d\eta$.

The number distribution then following from Eq. (2.9) is

$$\begin{aligned} \frac{1}{\sigma_{in}} \frac{d\sigma}{d\eta} &= \frac{dN}{d\eta} \\ &= \frac{N}{(2\pi L)^{1/2}} \int_0^\infty \frac{\xi^2 \exp[-\xi - y^2(\xi)/2L] d\xi}{(\xi^2 + \mu_1^2)^{1/2}}, \end{aligned} \quad (3.7)$$

where μ and $y(\xi)$ are defined by

$$\begin{aligned} \mu_1 &= B_1 m_\pi \operatorname{sech} \eta, \\ \tanh y(\xi) &= \frac{\xi}{(\xi^2 + \mu_1^2)^{1/2}} \tanh \eta. \end{aligned} \quad (3.8)$$

We shall evaluate this for various energies using Landau's predictions of the parameter L

$$L = \frac{1}{2} \ln(s/4m_p^2). \quad (3.9)$$

Here m_p is the proton mass. Table II gives the energy dependence of various parameters useful in the Landau model.

Figures 3 and 4 compare the input Gaussian with the resulting η distribution for $\sqrt{s} = 30.6$ and $\sqrt{s} = 53.0$, corresponding to energies actually used in ISR experiments, in particular the Pisa-Stony Brook experiment.²⁸ If we normalize to the exper-

imental area of the latter experiment, nearly perfect agreement is obtained with the curves reproduced in Jacob's rapporteur's talk² at the NAL conference.

An additional qualitative point exhibited by Figs. 3 and 4 is that the large- η distribution does not coincide with the large- y distribution. Therefore one cannot safely equate y with η even for large values of these variables.

Figure 5 shows the effect of increasing the particle mass; we have assumed $E = 1500$ GeV, $m = m_K$, $B_1 = 4.2$ ($m_K B = 2.06$), as seems appropriate for K mesons produced at ISR energies. The dip in the K distribution is less pronounced but still visible at NAL energies.

Figure 6 shows the predicted number distribution computed from Eq. (3.7) for pion parameters ($m_\pi B = 0.875$), normalized to the total charged multiplicity $N = 2.0 E^{1/4}$ (E measured in GeV). At 100 GeV there is no discernible flatness, while at the highest ISR energies (corresponding to $E = 1500$ GeV) the distribution is quite flat in the variable η . In the following section we shall discuss recent experimental data in the light of the present analysis.

c. The flattened Gaussian rapidity distribution. Another plausible rapidity distribution is a hybrid of the multiperipheral and Landau distribution, i.e., a flat-topped Gaussian. For instance we can adopt one of the curves of Fig. 3 or 6 as a rapidity distribution, feed it back into the integral (2.9) [using the factorized form (3.1)] and compute the resulting η distribution. Carrying this out for $E = 1500$ GeV gives the results shown in Fig. 7.

d. The laboratory η distribution. In order to compute the laboratory distribution $dN/d\eta_L$ we have only to express the c.m. expression in terms of lab variables since f is a Lorentz scalar [$f_L(p_L) = f(p) = f(\Lambda^{-1}p_L)$]. Hence $p_\perp = p_{\perp L} = p_L \operatorname{sech} \eta_L$ by Eq. (2.8), and $y = y_L - y_c$ by (2.2), where $y_c = \ln \gamma(1 + \beta)$ and β is the relative velocity of the c.m. and lab frames. Performing a calculation analogous to (3.7) leads to

TABLE II. Some basic parameters appearing in the hydrodynamical model are shown as a function of laboratory proton energy E . s is the total squared c.m. energy in pp collisions. L is the width of the Gaussian rapidity distribution of Eq. (1.5), and the total charged multiplicity is computed from the formula $2.0 E^{1/4}$, with E measured in GeV.

E (GeV)	50	100	200	300	400	500	1000	1500
s (GeV)	95.8	189.8	377.8	565.8	753.8	941.8	1881.8	2821.8
L	1.65	1.99	2.34	2.54	2.68	2.79	3.14	3.34
N	5.31	6.32	7.52	8.34	8.93	9.45	11.26	12.46

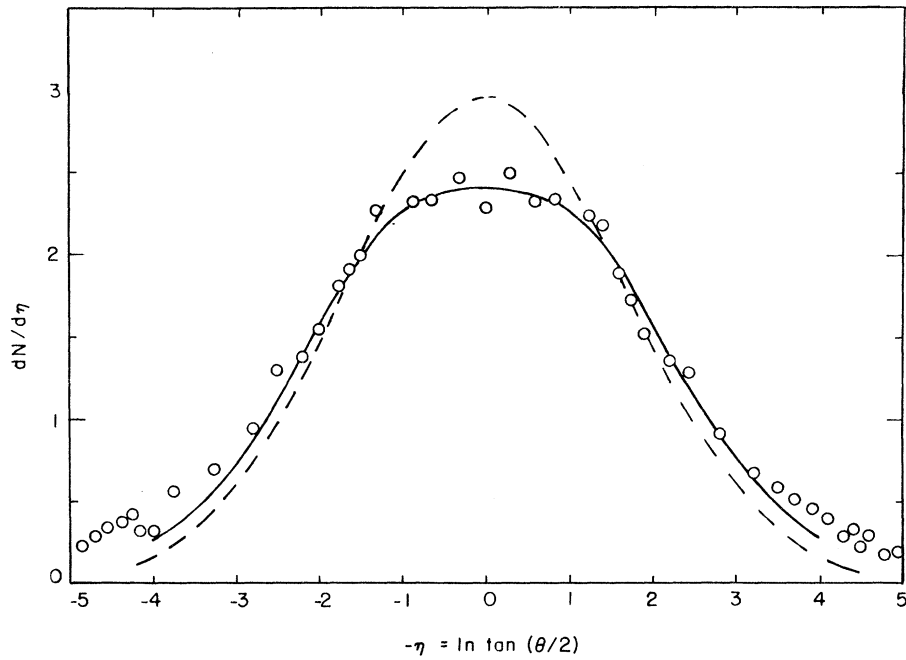


FIG. 3. The difference between distributions in the rapidity variable y and the cosmic-ray variable $\eta = -\ln \tan(\theta/2)$ is illustrated in this c.m. number distribution for $s = 936 \text{ GeV}^2$ ($E = 497 \text{ GeV}$). The solid curve is the distribution $dN/d\eta$ computed using Eq. (3.7) when the rapidity distribution is a Landau Gaussian. The peak in $|y| < 1$ is flattened whereas the wings are broadened. Data points are from Ref. 28.

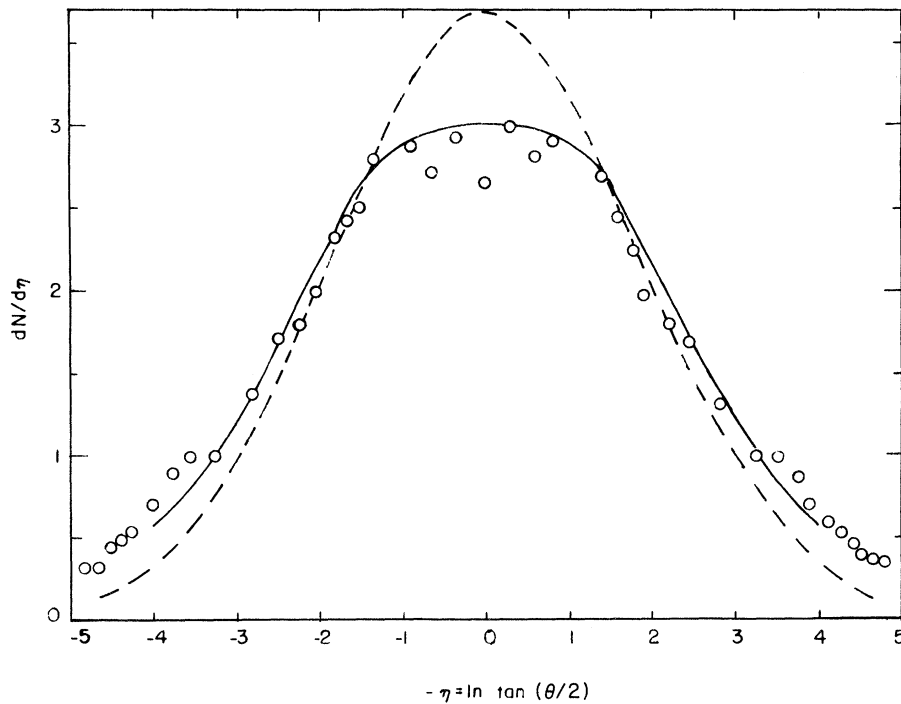


FIG. 4. This figure is the same as Fig. 3 except that the energy has been increased to $s = 2809 \text{ GeV}^2$ ($E = 1493 \text{ GeV}$). The central region is broader and flatter (in the variable η) than in Fig. 3. The normalization is chosen to agree with Ref. 28.

$$\begin{aligned} \frac{1}{\sigma_{\text{in}}} \frac{d\sigma}{d\eta_L} &= \frac{dN}{d\eta_L} \\ &= \frac{N}{(2\pi L)^{1/2}} \int_0^\infty \frac{\xi^2 e^{-\xi}}{(\xi^2 + \mu_1^2)^{1/2}} \\ &\quad \times \exp[-(y_L - y_c)^2/2L] d\xi, \end{aligned} \quad (3.10)$$

$$\mu_1 = mB_1 \operatorname{sech} \eta_L.$$

In order to compare with the 205-GeV NAL experiment²¹ we take $N=7.65$ (very close to the Fermi-Landau formula $2.0 E^{1/4}$), and $m_\pi B = 0.875$, and evaluate L ($L=2.35$) using Eq. (3.9). The resulting curve (Fig. 8) shows excellent agreement with the data. These data do not as yet exclude a small flat region near the peak, yet the general skewed Gaussian behavior of the experimental points is nicely accounted for by (3.10).

The systematic energy dependence of (3.10) is exhibited in the predictions of the total charged multiplicity in Fig. 9. In computing this curve we computed L using Eq. (3.9) and used the multiplicity formula $2.0 E^{1/4}$. (The latter is easily corrected to other normalizations by an appropriate scale factor.) Pion parameters were used ($m_\pi B = 0.875$) but this approximation should not be a significant source of error.

The calculations of Secs. III B and III D were all done with the simple exponential transverse momentum distribution of Eq. (2.12). It is of interest to compare some of these predictions with those resulting from the Gaussian (2.13) or with sums of Gaussians

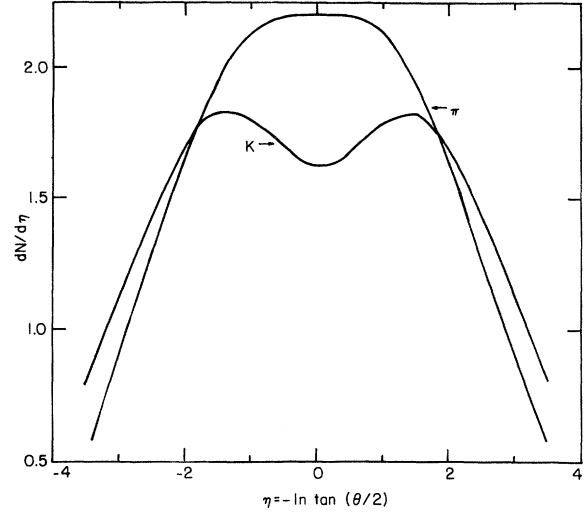


FIG. 5. The π and K η distributions (normalized to the same total area) are given at $E=1500$ GeV to show the effect of changing the particle mass. In each case the rapidity distribution was assumed to be a Landau Gaussian. For the π curve we took $m_\pi B_1 = 0.875$ and for the K curve $m_K B_1(K) = 2.06$ [corresponding to $B_1(K) = 4.2 \text{ GeV}^{-1}$].

$$\begin{aligned} f_3(p) &= \sum_{i=1}^N \alpha_i \beta_i^2 \exp(-B_i^2 p^2), \\ \sum_{i=1}^N \alpha_i &= 1. \end{aligned} \quad (3.11)$$

We adopt the criterion that $\langle v \rangle$ at 90° should be the same in order to see the effect of the difference in shape. For comparison of a single expo-

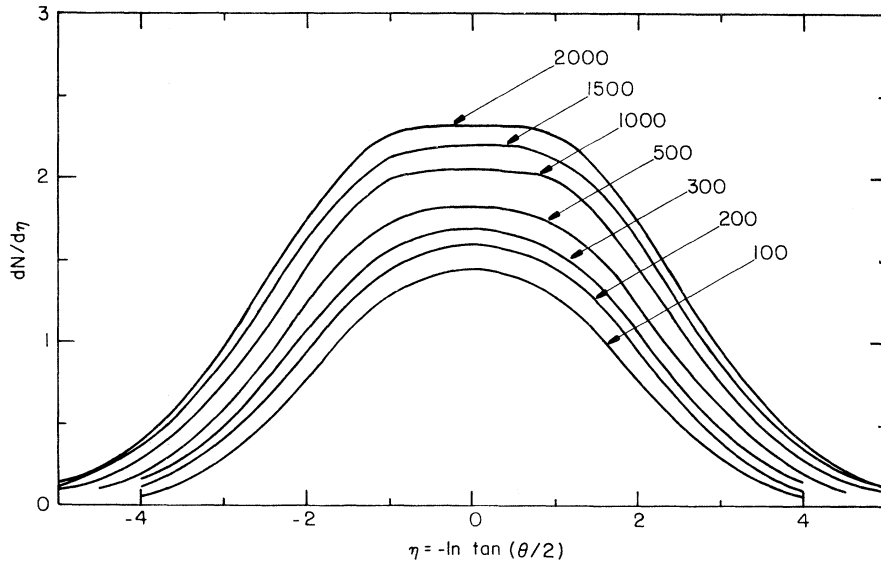


FIG. 6. Predictions of the c.m. number distribution $dN/d\eta$ from Eq. (3.7) are shown for lab energies E (in GeV) appropriate to the NAL and ISR facilities. Note that the flatness becomes more pronounced as the energy increases. Pion parameters are used ($m_\pi B = 0.875$) and the multiplicity is assumed to be $2.0 E^{1/4}$.

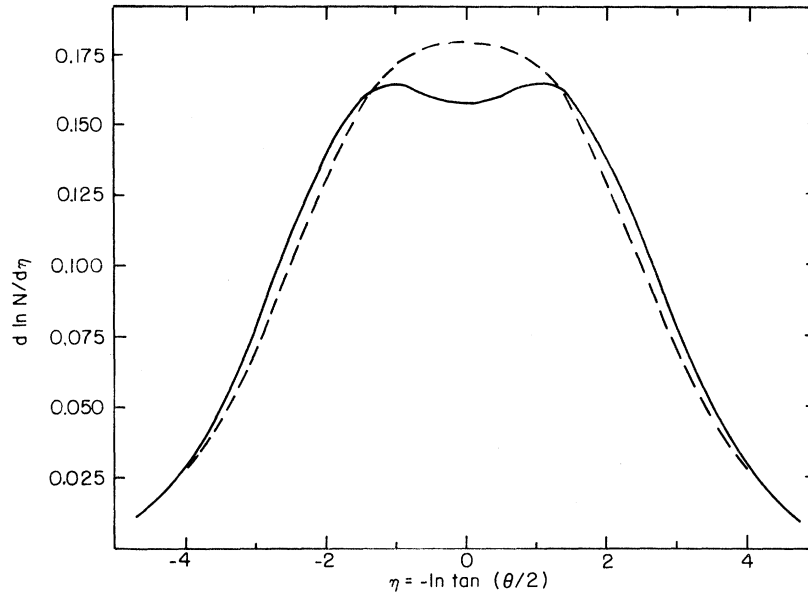


FIG. 7. In order to see the qualitative behavior of the c.m. η distribution $(1/N)dN/d\eta$ when the rapidity distribution is flattened in the center we have used the output curve (dashed) $(1/N)(dN/d\eta)_{\eta=y}$ as the input rapidity distribution in Eq. (3.7) instead of the Gaussian. Pion parameters were again used in this calculation.

nential with $B_1 = 6.25 \text{ (GeV/c)}^{-1}$ we have $B_2^2 = 12.1$ (cf. Table I). The c.m. formula for $dN/d\eta$ is exactly like (3.7) except for the change of $e^{-\xi}$ to $2e^{-\xi^2}$. The two distributions are compared in Fig. 10 for $E = 500 \text{ GeV}$.

IV. IS THE RAPIDITY DISTRIBUTION FLAT IN THE CENTRAL REGION?

We are now prepared to analyze recent experimental results in the light of the investigation of

Sec. III. Although many experimental groups have announced the (theoretically desired) result that the rapidity distribution has a plateau in the central region at ISR energies, we shall find these results to be contradictory and confusing when subjected to careful analysis. Some groups^{29,30} have found flat η distributions (and then over a rather small range of η), while others³¹⁻³⁴ give y distributions for various fixed p_{\perp} . In the latter case possibly nonconstant cross sections are often ren-

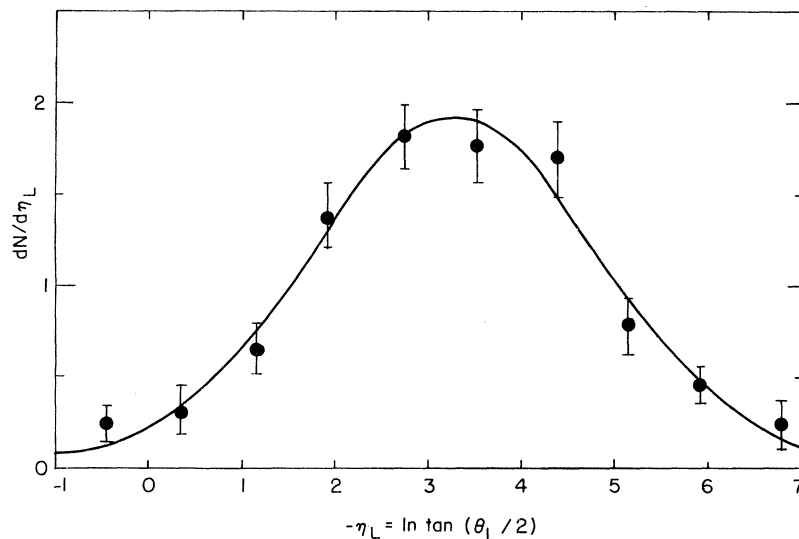


FIG. 8. The laboratory distribution $dN/d\eta_L$ is computed using Eq. (3.10) and compared to the 205-GeV data of Ref. 21. If the parameter m (we used $m_{\pi}B = 0.875$) is known and the multiplicity fixed at any energy, there are no adjustable constants in the model.

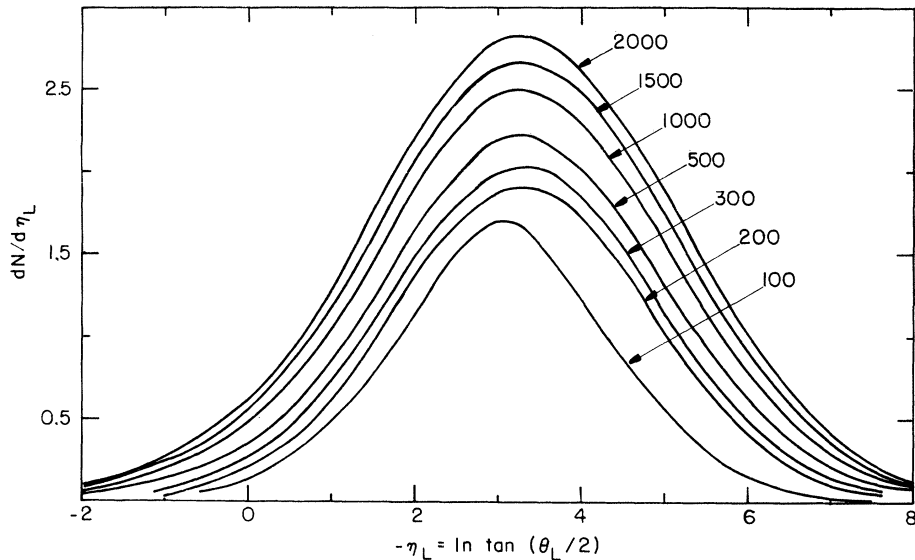


FIG. 9. The systematic energy dependence of the laboratory distribution $dN/d\eta_L$ according to Eq. (3.10) is shown. Pion parameters ($m_\pi B = 0.875$) were used and the curves are normalized to a total charged multiplicity $N = 2.0 E^{1/4}$ (E is the lab proton energy in GeV).

dered flat by using logarithmic graph paper and a stretched-out horizontal scale. Moreover, some authors have evidently³⁵ assumed the equivalence of the variables, if not in the analysis then in the description of the analysis.

Hence we need to inspect the consistency of various experiments and then to adopt a rational criterion for flatness (rational means uncolored by prejudice based on some theoretical model).

We first consider the results of Barbiellini *et*

al.,²⁹ who give the total charge distribution $dN/d\eta$ in the c.m. frame at $s = 915, 2000,$ and 2800 GeV^2 . The η distributions obtained by this group are essentially constant in the (small) interval $0 < |\eta| < 0.8$. These authors claim that their results are compatible with a flat rapidity distribution and a Gaussian p_\perp distribution $\exp(-B^2 p_\perp^2)$ for $3 < B^2 < 18 (\text{GeV}/c)^{-2}$. Our calculations (cf. Fig. 2) show that the range of η in this experiment is not great enough to be sensitive to the shape of the rapidity

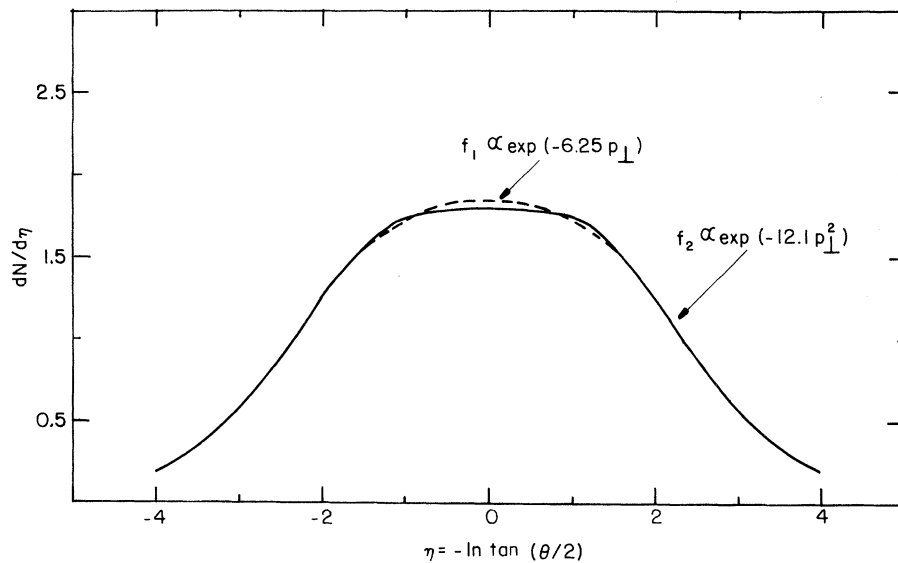


FIG. 10. In order to examine the effect of the detailed shape of the transverse momentum distribution on $dN/d\eta$ we have computed $(1/N)(dN/d\eta)$ for the distributions (2.12) and (2.13), adjusted to give the same $\langle v \rangle$ at 90° in the c.m. frame [consequently $(dN/d\eta)_1 = (dN/d\eta)_2$ for $\eta = 0$]. The values of B_i are $B_1 = 6.25, B_2^2 = 12.1$.

distribution. A detailed comparison with the data is made in Fig. 11, showing that one cannot experimentally distinguish the flat y distribution from the Landau Gaussian distribution. Also shown are the predictions of the Landau distribution of Eq. (3.7), again normalized by eye.

The results of Breidenbach *et al.*³⁰ are very similar to those of the foregoing group. If anything, these data indicate an even flatter η distribution over a larger range of η ($0 < |\eta| < 1.3$), although in some cases the scatter seems to be substantial. Figure 12 shows the data compared with the predicted distributions following from flat and Landau Gaussian rapidity distributions for exponential p_{\perp} distributions of the form $\exp(-6.25 p_{\perp})$. The reader can judge for himself which fit he prefers.

It is also necessary to mention the compilation of Fig. 8 in the review paper of Sens.³⁵ The figure in question summarizes an attempt to piece together various experimental results available at the time. This synthesis is quite reasonable except for the crucial matter of how one treats the central region. We find agreement with the central points only if the variable is η , not y . In y ,

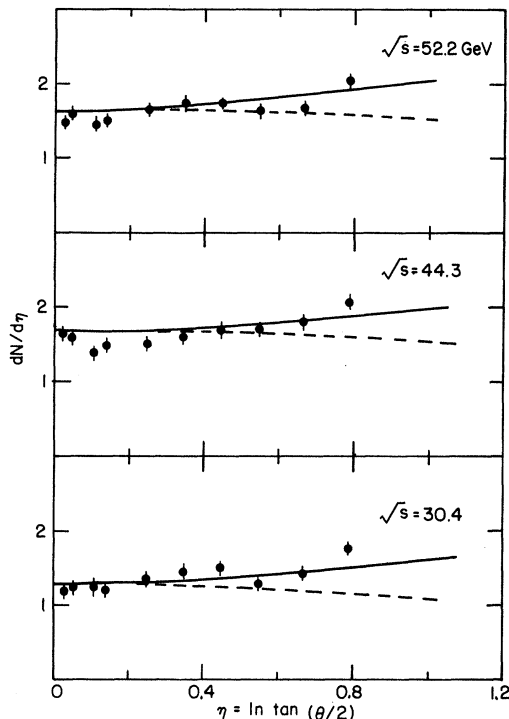


FIG. 11. The data of Barbiellini *et al.* (Ref. 29) are compared with η distributions calculated using a flat rapidity distribution (solid line) and a Landau Gaussian rapidity distribution (dashed lines). In each case the transverse distribution was taken to be $\exp(-6.25 p_{\perp})$ and the height adjusted to please the eye. It is difficult to choose between the two cases.

the central points computed from the data of Breidenbach *et al.*³⁰ should be $1/\langle v \rangle \approx 25\%$ higher. With this correction much of the convincing evidence for a central plateau disappears.

The foregoing criticisms are made with the realization that the range of η is very small in the first two experiments and, more importantly, that the experimental errors could be much bigger than statistical.

Now we turn to the results of the British-Scandinavian collaboration,²² which should be superior to the foregoing experiments for our purposes since momentum is measured, making possible a determination of true rapidity. The results at $\sqrt{s} = 30.4$ GeV are given for $p_{\perp} = 0.2, 0.4, 0.6, 0.8, 1.0$, and appear quite flat to the naked eye except for the larger values of p_{\perp} . This constancy is partly due to the fact that the data are indeed slowly varying and partly due to the use of log scale for

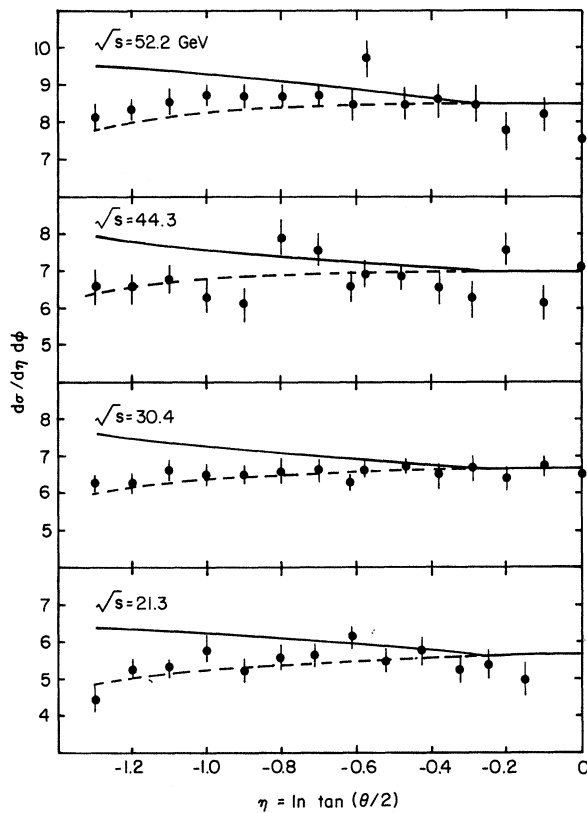


FIG. 12. The data of Breidenbach *et al.* (Ref. 30) are compared with η distributions calculated using a flat rapidity distribution (solid line) and a Landau Gaussian rapidity distribution (dashed line). In each case the transverse distribution was taken to be $\exp(-6.25 p_{\perp})$ and the height adjusted to please the eye. In contrast to the data of Fig. 11 (which cover a smaller range of η) the Gaussian rapidity distribution gives a distinctly better fit.

the vertical axis and an expanded scale for the horizontal axis. Numerical integration to obtain $d\sigma/dy$ shows that there is a 23% decrease as y goes from 0 to 1.1. This is to be compared with a 19% decrease predicted by the Landau formula at this energy. Some might consider this flat enough, but the visual appearance of the complete Gaussian distribution will never be flat, even though the percent decrease in a *fixed* rapidity interval $0 < |y| < c$ will get smaller and smaller as s increases.

The same group has produced²² similar data at the higher energy $s = 2000 \text{ GeV}^2$, but without the crucial (dominant) value $p_{\perp} = 0.2$. These data have a flat appearance, and if the $p_{\perp} = 0.2$ region is also flat one might conclude that a plateau is indeed developing at this very high energy. Of course this result then contradicts the flat η distributions found in Refs. 29 and 30 at the same energy.

On the basis of the foregoing analysis it appears that current evidence is inconclusive on the theoretically interesting question of the shape of the rapidity distribution in the central region. It is also apparent that the y dependence of $Ed^3\sigma/d^3p$ is somewhat greater for large p_{\perp} than for small p_{\perp} . This fact, apparent at both ISR and conventional energies, means that factorized distributions of the form (3.1) are too simple to account for the facts. Of course (3.1) represents^{9,18} only the leading term in the hydrodynamical model. We plan to discuss these second-order questions elsewhere. In the present work we are primarily concerned with integrated distributions, which depend less on the fine details of the double differential cross section.

V. FURTHER REMARKS ON THE GAUSSIAN RAPIDITY DISTRIBUTION

The possible experimental fact of a Gaussian rapidity distribution of produced particles is significant independently of the Landau model. (The authors are confident that at least some of the contemporary models are sufficiently flexible to produce such distributions.) Only further detailed calculations of correlations and other fine structure can be expected to establish (or disprove) the hydrodynamic picture of particle production.

In the present section we examine various reactions (including πp , Kp , and γp as well as pp collisions) and find widespread evidence for Gaussian distributions of charged secondaries, even at energies so low that no justification for statistical methods can be given. For unlike particles the forward-backward symmetry characteristic of pp collisions is no longer expected. Therefore, we shall compare data with the formula

$$\frac{1}{\sigma_{\text{in}}} \frac{d\sigma}{dy} = N \exp[-(y - y_0)^2/2L] / (2\pi L)^{1/2} \quad (5.1)$$

in order to determine the best values of y_0 and L . In order to expedite the fit we take the logarithm of (5.1), giving a quadratic

$$\ln\left(\frac{d\sigma}{dy}\right) = K - (y - y_0)^2/2L, \quad (5.2)$$

which is matched to the data using a least-squares routine. The constant K is

$$K = \ln N\sigma_{\text{in}} - \frac{1}{2} \ln(2\pi L), \quad (5.3)$$

and can be used as a check on $N\sigma_{\text{in}}$ if desired. Thus we want to choose K, L, y_0 to minimize

$$M(K, L, y_0) = \sum_i \left[\ln\left(\frac{d\sigma}{dy}\right)_i - \left(K - \frac{(y_i - y_0)^2}{2L} \right) \right]^2. \quad (5.4)$$

Here y_i are the points at which the $(d\sigma/dy)_i$ are measured. We can also fit this to $d^2\sigma/dp_{\perp} dy$ for fixed p_{\perp} ; in this case it turns out that, at least at BNL energies, L decreases with increasing p_{\perp} . This effect also appears to occur at higher (ISR) energies, as mentioned in Sec. IV.

Full rapidity distributions are surprisingly scarce at present. We treat the following data: (1) $\gamma p \rightarrow \pi^- X$ for³⁶ $E_{\gamma} = 2.8, 4.7, \text{ and } 9.3 \text{ GeV}$; (2) $\pi^+ p \rightarrow \pi^- X$ at³⁷ $7 \text{ GeV}/c$ and³⁸ $18.5 \text{ GeV}/c$; (3) $K^+ p \rightarrow \pi^- X$ at $12.7 \text{ GeV}/c$.³⁷

For $\pi^+ p \rightarrow \pi^- X$ ($7 \text{ GeV}/c$) the results are $y_0 = 0.26$, $L = 0.71$ [note that the formula (1.6) gives $L = 0.72$]; for $\pi^+ p \rightarrow \pi^- X$ ($18.5 \text{ GeV}/c$) $y_0 = 0.20$, $L = 1.07$ compared with $L = 1.17$ from (1.6). For $K^+ p \rightarrow \pi^- X$ ($12.7 \text{ GeV}/c$) the fit gives $y_0 = 0.25$, $L = 0.95$, while $L = 0.99$ from Eq. (1.6). Next, consider $\gamma p \rightarrow \pi^- X$; the values of (y_0, L) at $E_{\gamma} = 2.8, 4.7, \text{ and } 9.3 \text{ GeV}$ are $(0.35, 0.65)$, $(0.38, 0.85)$, $(0.46, 1.00)$. Since we have not given a theory of collisions of unlike particles, it is not completely clear that the L of Eq. (1.6) should be reliable, especially at the relatively low energies in the experiments cited above.

There have been interesting speculations on displacements of the peak based on the idea that the quark c.m. frame is preferred for the description of particle production.³⁹ In the context of the hydrodynamical model a similar problem has been studied, i.e., the asymmetry in nucleon-nucleus collisions.^{4,9,11} (In that case it appears that the equal-velocity frame is preferred.) Thus far nobody has investigated the prediction of the hydrodynamical model for the collision of unlike particles, although it is unlikely that the dynamics would change much on replacing one hadron by another. Moreover, the similarity of photon-induced

reactions to purely hadronic reactions, with regard to both the multiplicity (also $2.0 E^{1/4}$; see Ref. 36) and rapidity distributions, suggests that ρ dominance could account for the principal features of this process. Figure 13 shows the empirically determined energy dependence of $a = 1/2L$, compared with Landau's formula $L = \frac{1}{2} \ln(s/4m^2)$. The integrated cross sections give L values which agree too well with this formula. [The fixed- p_{\perp} fits give p_{\perp} -dependent values of L which contradict the factored form of Eq. (3.1) at BNL energies, although the integrated or average behavior has the correct L .]

It is entirely likely, as suggested by Cooper,⁴⁰ that the " p_{\perp} dependence of L " at moderate energies is really due to a kinematic effect, namely that y_{\max} decreases with increasing p_{\perp} and that formula (3.6) ignores this fact. One could introduce an *ad hoc* envelope function decreasing to zero on the phase-space boundary, which has essentially the same effect. In the present work our main interest is in extremely high energies, so we shall not pursue this question further. Even at the lower energies the amount of cross section involved is very small.

The detailed form of L is, after all, asymptotic and is based on a slablike initial condition. The formula could easily be $L = A \ln(s/4m^2) + B$, with $A \neq \frac{1}{2}$ and $B \neq 0$. In fact, B is not negligible in some treatments of this problem.⁹ Secondly, the energy actually available to the secondaries is not the total energy because of the leading-particle effect. Suppose¹⁸ the energy available to the expanding hadronic matter is ks , where $k \approx \frac{1}{2}$. Then L is de-

creased by $\frac{1}{2} \ln k$, which is $\approx -\frac{1}{2} \ln 2 \approx -0.35$. This is a rather small correction; typical L values are 2 to 4 in this paper. Also striking is the fact⁴¹ that the four-prong events in 6.6 GeV/c pp collisions have a rapidity distribution in perfect agreement with the Landau Gaussian and the theoretical width L .

At the lower energies there is considerable dependence on the charge of the selected final particle. For instance, at 24 GeV the $pp \rightarrow \pi^- X$ data of Mück *et al.* are much smoother and better fitted by a Gaussian than are the $pp \rightarrow \pi^+ X$ data. This is scarcely surprising in view of the many dynamical effects associated with the phenomenon of the leading proton.

VI. A NEW ENERGY-DEPENDENT SCALING LAW

We return to the c.m. rapidity distribution

$$\frac{1}{N} \frac{dN}{dy} = \exp(-y^2/2L)/(2\pi L)^{1/2} \quad (6.1)$$

for charged-particle production in pp collisions. As we have seen, this simple formula gives a good approximate description of many experiments, at least up to the highest available ISR energies at which the rapidity distribution may be somewhat flatter than (6.1) near $y=0$. It is possible to cast (6.1) in a simple universal form⁵ by defining the variable z :

$$z = y/\sqrt{L} . \quad (6.2)$$

Now Eq. (6.1) becomes

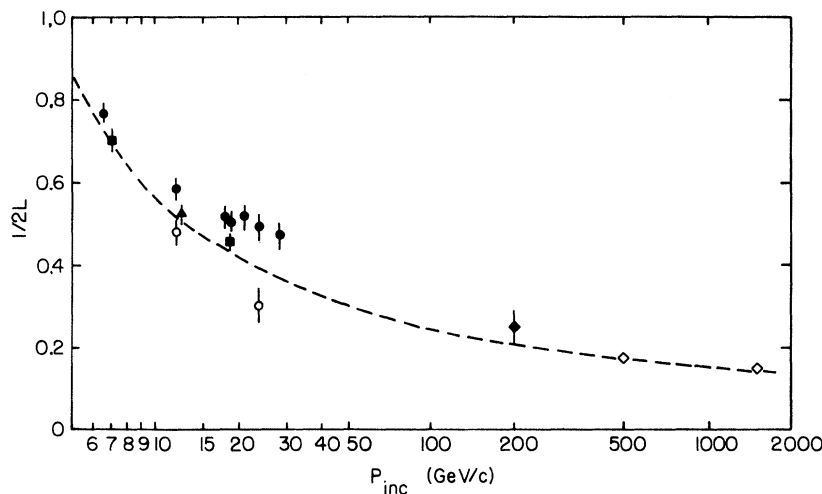


FIG. 13. The experimental energy dependence of $1/2L$ [obtained from a least-squares fit to the Gaussian $\exp(-y^2/2L)$ to $d\sigma/dy$] is shown. The theoretical prediction of Eq. (1.6) is given by the dashed curve. Solid circles correspond to $pp \rightarrow \pi^- X$ (from Refs. 24, 25, 31, 41, and 42). Open circles correspond to $pp \rightarrow \pi^+ X$ (from Ref. 31). Triangles correspond to $K^+ p \rightarrow \pi^- X$ (from Ref. 26). Squares correspond to $\pi^+ p \rightarrow \pi^- X$ (from Refs. 26 and 38). Solid diamonds correspond to $pp \rightarrow N_{\text{ch}} X$ (from Ref. 21). Open diamonds correspond to $pp \rightarrow N_{\text{ch}} X$ (from Ref. 2).

$$\frac{1}{N} \frac{dN}{dz} = \frac{e^{-z^2/2}}{(2\pi)^{1/2}}, \quad (6.3)$$

which formula boldly lacks any adjustable constants, except to fix the constant K in the multiplicity formula $N=KE^{1/4}$.

This (energy-dependent) scaling law is conveniently written in the form

$$\ln\left(\frac{N}{dN/dz}\right) = \frac{1}{2}z^2 + \frac{1}{2}\ln(2\pi). \quad (6.4)$$

Hence the use of the variable z is supposed to remove the energy dependence from the rapidity distribution.

Figure 14 shows various data^{24,25,31,42} plotted as a function of z . The over-all agreement is quite good.

VII. ENERGY DEPENDENCE OF THE ANGULAR DISTRIBUTION IN THE CENTRAL REGION

Equation (6.1) is closely connected with the angular distribution $d\sigma/d\Omega$ in the central region, where $d\sigma/d\eta$ is a constant $\langle v \rangle$ times $(d\sigma/dy)_{y=0}$ over a range of y (cf. Fig. 6). Throughout this range of η [typically $O(1)$ at ISR energies] we have^{29,30}

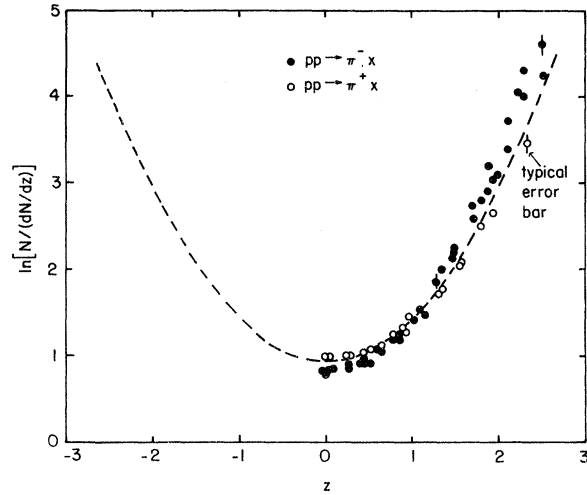


FIG. 14. Plot of $\ln[N/(dN/dz)]$ as a function of $z = y/\sqrt{L}$. The dashed parabola is the prediction of Eq. (6.4). For the momenta of 19, 21, and 28.5 GeV/c, we have made use of existing curves for $d\sigma/dy$ (Refs. 24, 25, 41, and 42). For the momenta of 12 and 24 GeV/c, we have integrated the published curves (Ref. 31) $(1/\pi)d^2\sigma/dy dp_{\perp}^2$ over all given p_{\perp} to get $d\sigma/dy$. Note that the π^- data ($pp \rightarrow \pi^- X$) cluster on the inside of the universal curve for $z > 0.75$, while the π^+ data cluster on the outside. Other data (including those from ISR) were plotted in this manner in Ref. 5.

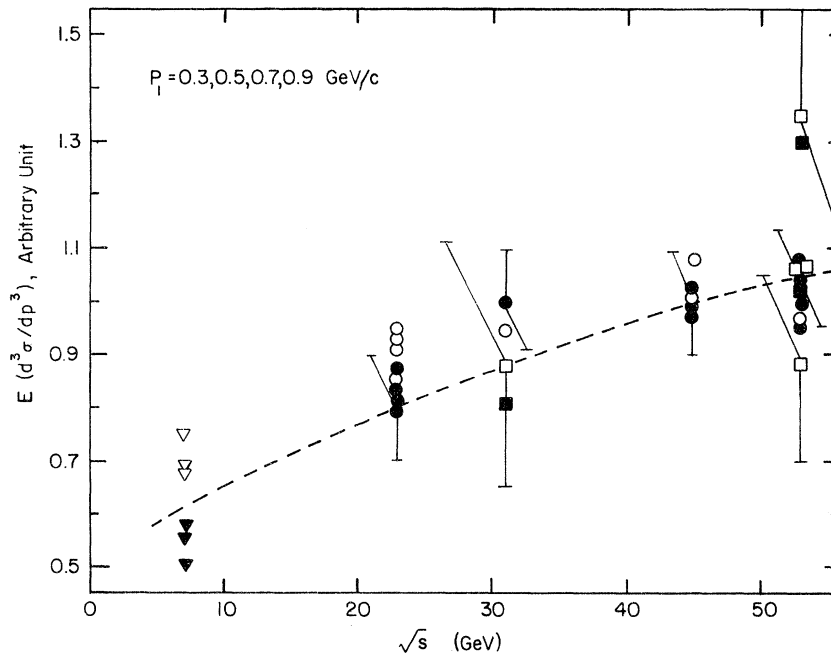


FIG. 15. Plot of the 90° c.m. inclusive cross section $E d^3\sigma/dp^3$ for $pp \rightarrow \pi^+ X$ as a function of \sqrt{s} . π^+ data are shown as open points and π^- data are shown as solid points. The data appearing in cited references were plotted for each p_{\perp} separately. Here we combined them in one plot, and for each p_{\perp} , $E d^3\sigma/dp^3$ was normalized to unity at $\sqrt{s} = 43$ GeV. The dashed curve is the theoretical prediction, where $E d^3\sigma/dp^3$ varies with energy as $(\gamma_{c.m.}/\ln\gamma_{c.m.})^{1/2}$, normalized the same way as the experimental curves. Data points are taken from Refs. 31 (triangles), 22 (circles), and 35 (squares).

$$\frac{d\sigma}{d\Omega} \cong \frac{A(s)}{\sin^2\theta}, \quad (7.1)$$

where $A(s)$ is given by⁵

$$A(s) = \frac{N\langle v \rangle \sigma_{in}}{(2\pi)^{3/2} [\ln(s/4m_p^2)]^{1/2}} \sim \frac{s^{1/4}}{[\ln(s/4m_p^2)]^{1/2}}. \quad (7.2)$$

The $\sin^{-2}\theta$ angle dependence of (7.1) is in agreement with Refs. 29 and 30 and presumably in disagreement with the flat y distribution at $\sqrt{s} = 53$ GeV reported in Ref. 22. In order to check the (nonscaling) energy dependence of (7.2) we plot in Fig. 15 the energy dependence of the 90° cross section. Although the energy dependence is very well explained, the numerical value of $A(s)$ seems to be slightly too high, i.e., $\langle v \rangle$ determined by the fit to the data is ~ 0.6 rather than the ~ 0.8 expected from the empirical p_\perp distribution.

The approximate $s^{1/4}$ dependence has been noted independently as an empirical rule.⁴³ Of course, (7.2) implies that the *possibly hypothetical* scaling "limit" is never reached in the central region. The result, (7.2), which is simple and natural in the Landau approach, is awkward (and involves constants which are arbitrary or have the wrong sign) in Regge or multiperipheral models.

VIII. APPROXIMATE FEYNMAN SCALING; DEVIATIONS FROM SCALING AT SMALL x

It remains to relate the Landau model to "Feynman scaling." Although the Feynman variable x defined by²⁰

$$x = 2p_\parallel / \sqrt{s} \quad (8.1)$$

is not at all natural in a model in which the natural coordinates are y and p_\perp , it happens that except for very small x (where scaling is in doubt) the Landau distribution (3.6) automatically gives approximately energy-independent x distributions. However, this result appears purely fortuitous, and the variable x presently appears to be unnatural from the point of view of the hydrodynamical model.

From Eq. (2.1) we see that x and y are related by

$$y = \frac{1}{2} \ln \left(\frac{(x^2 + 4m_\perp^2/s)^{1/2} + x}{(x^2 + 4m_\perp^2/s)^{1/2} - x} \right), \quad (8.2)$$

where $m_\perp^2 = m_\pi^2 + p^2$ for pions.

For factored distributions of the Landau type [(3.6)] we have

$$\frac{d^2N}{dx dp_\perp} = p_\perp f_i(p_\perp) F(x, p_\perp, s), \quad (8.3)$$

where $f_i(p_\perp)$ is one of the distributions (2.12) or

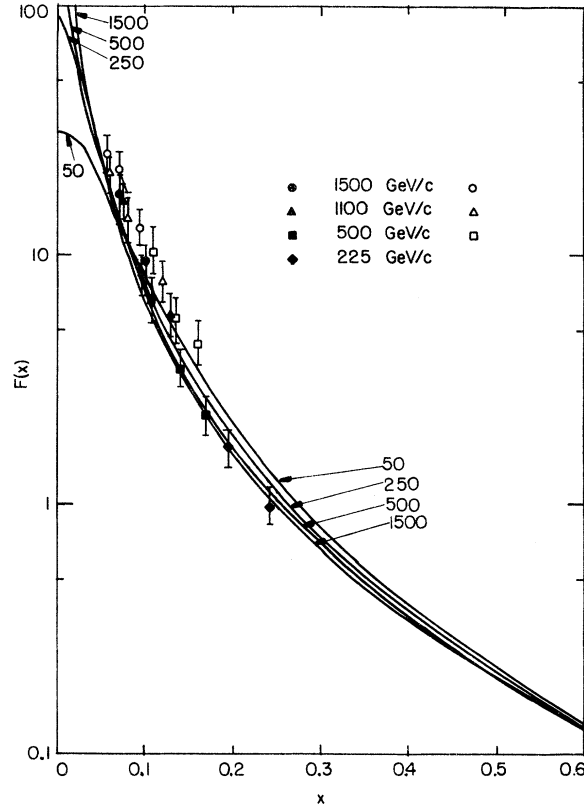


FIG. 16. The hydrodynamical model gives approximate scaling in the variable x except for very small x where significant deviations are predicted. The dependence of the distribution $F(x, p_\perp, s)$ of Eq. (8.4) is shown for $p_\perp = 0.2$ for various equivalent laboratory proton energies. The data are taken from Refs. 32, 33, and 45.

(2.13), and $F(x, p_\perp)$ is

$$F(x, p_\perp, s) = \frac{N \exp[-y^2(x, p_\perp)/2L]}{(2\pi L)^{1/2} (x^2 + 4m_\perp^2/s)^{1/2}}. \quad (8.4)$$

Figure 16 shows $F(x, 0.2, s)$ for a wide range of lab proton energies. Scaling is approximately valid for $x > 0.05$. The experimental tendency of low-energy x distributions to cross over the high-energy x distributions was already noted by Panvini *et al.*⁴⁴ The characteristic prediction of the hydrodynamical model (or any model giving rapidity Gaussians) is that the x distributions become increasingly peaked for small x as the energy increases. Hence we expect scaling to break down in a very specific way for $x < 0.05$. Similar results have been found by Cooper and Schonberg.¹⁸

ACKNOWLEDGMENTS

The authors are indebted to Dr. Lucy Carruthers for considerable help with the numerical computation. We also wish to acknowledge helpful conversations with F. Cooper, J. Ellis, and D. Horn.

*Work supported in part by the National Science Foundation.

†Present address: Los Alamos Scientific Laboratory, Los Alamos, New Mexico 87544.

¹D. Horn, Phys. Rep. 4C, 1 (1972).

²M. Jacob, in *Proceedings of the Sixteenth International Conference on High Energy Physics, National Accelerator Laboratory, Batavia, Ill., 1972*, edited by J. D. Jackson and A. Roberts (NAL, Batavia, Ill., 1973), Vol. 3, p. 373.

³A. H. Mueller, in *Proceedings of the Sixteenth International Conference on High Energy Physics, National Accelerator Laboratory, Batavia, Ill., 1972*, edited by J. D. Jackson and A. Roberts (NAL, Batavia, Ill., 1973), Vol. 1, p. 347.

⁴L. D. Landau, Izv. Akad. Nauk SSSR 17, 51 (1953); L. D. Landau and S. Z. Belen'kij, Usp. Fiz. Nauk 56, 309 (1955); Nuovo Cimento Suppl. 3, 15 (1956). These articles have been reprinted (in English translation) in *Collected Papers of L. D. Landau*, edited by D. Ter Haar (Gordon and Breach, New York, 1965).

⁵P. Carruthers and Minh Duong-van, Phys. Lett. 41B, 597 (1972).

⁶E. Fermi, Prog. Theor. Phys. 5, 570 (1950); Phys. Rev. 81, 683 (1951).

⁷G. A. Milekhin, in *Proceedings of Moscow Cosmic Ray Conference, 1960*, edited by N. M. Gerasimova (VINITI, Moscow), Vol. 1, p. 220.

⁸A. A. Emel'yanov, in *Proceedings of the P. N. Lebedev Physics Institute*, edited by D. V. Skobel'tsyn (Consultants Bureau, New York, 1967), Vol. 29, p. 163.

⁹G. A. Milekhin, Zh. Eksp. Teor. Fiz. 35, 1185 (1958) [Sov. Phys.-JETP 8, 829 (1959)].

¹⁰I. L. Rozental', Zh. Eksp. Teor. Fiz. 31, 278 (1956) [Sov. Phys.-JETP 4, 217 (1957)].

¹¹S. Amai, H. Fukuda, C. Iso, and M. Sato, Prog. Theor. Phys. 17, 241 (1957).

¹²Z. Koba, Prog. Theor. Phys. 17, 288 (1957).

¹³M. Namiki and C. Iso, Prog. Theor. Phys. 18, 591 (1957).

¹⁴H. Ezawa, Y. Tomozawa, and H. Umezawa, Nuovo Cimento 5, 810 (1957).

¹⁵D. Ito and H. Tanaka, Nuovo Cimento Suppl. VII, 91 (1958).

¹⁶C. Iso, K. Mori, and M. Namiki, Prog. Theor. Phys. 22, 403 (1959).

¹⁷S. N. Ganguli and P. K. Malhotra, Phys. Lett. 42B, 83 (1972).

¹⁸F. Cooper and E. Schonberg, Phys. Rev. Lett. 30, 880 (1973).

¹⁹D. E. Lyon, C. Risk, and D. M. Tow, Phys. Rev. D 3, 104 (1971); R. N. Cahn, LBL Report No. LBL-1007, 1972 (unpublished).

²⁰R. P. Feynman, Phys. Rev. Lett. 23, 1415 (1969); also in *High Energy Collisions*, edited by C. N. Yang *et al.* (Gordon and Breach, New York, 1970).

²¹G. Charlton *et al.*, contribution to the Sixteenth International Conference on High Energy Physics, National Accelerator Laboratory, Batavia, Ill., 1972 (unpublished), and private communication from Dr. L. G. Hyman.

²²E. Lillethun, in *Proceedings of the Fourth International Conference on High Energy Collisions, Oxford, 1972*, edited by J. R. Smith (Rutherford High Energy Laboratory, Chilton, Didcot, Berkshire, England, 1972), Vol. 2, p. 197; in *Proceedings of the Sixteenth International Conference on High Energy Physics, National Accelerator Laboratory, Batavia, Ill., 1972*, edited by J. D. Jackson and A. Roberts (NAL, Batavia, Ill., 1973), Vol. 1, p. 211.

²³G. Giacomelli, in *Multiparticle Phenomena and Inclusive Reactions*, edited by J. Tran Thanh Van, 1972, Vol. 2, p. 275.

²⁴W. Sims *et al.*, Nucl. Phys. B41, 317 (1972).

²⁵H. Bøggild *et al.*, Nucl. Phys. B27, 1 (1971).

²⁶W. R. Frazer *et al.*, Rev. Mod. Phys. 44, 284 (1972).

²⁷K. Wilson, Cornell University Report No. CLNS-131, 1970 (unpublished).

²⁸Pisa-Stony Brook Collaboration, contribution to the Sixteenth International Conference on High Energy Physics, National Accelerator Laboratory, Batavia, Ill., 1972 (unpublished).

²⁹G. Barbiellini *et al.*, Phys. Lett. 39B, 294 (1972).

³⁰M. Breidenbach *et al.*, Phys. Lett. 39B, 654 (1972).

³¹H. J. Mück *et al.*, Phys. Lett. 39B, 303 (1972).

³²A. Bertin *et al.*, Phys. Lett. 38B, 260 (1972).

³³L. G. Ratner *et al.*, Phys. Rev. Lett. 27, 68 (1971).

³⁴Saclay-Strasbourg collaboration, reported in Ref. 35.

³⁵J. C. Sens, in *Proceedings of the Fourth International Conference on High Energy Collisions, Oxford, 1972*, edited by J. R. Smith (Rutherford High Energy Laboratory, Chilton, Didcot, Berkshire, England, 1972), Vol. 1, p. 177.

³⁶K. C. Moffeit *et al.*, Phys. Rev. D 5, 1603 (1972).

³⁷M. E. Law *et al.*, Particle Data Group Report No. LBL-80, 1972 (unpublished); p. 691 gives results from the BNL-Wisconsin collaboration (unpublished).

³⁸W. D. Shephard *et al.*, Phys. Rev. Lett. 28, 703 (1972).

³⁹H. Satz, Phys. Rev. Lett. 19, 1453 (1967).

⁴⁰F. Cooper (private communication).

⁴¹E. Gellert (unpublished).

⁴²E. Berger, Y. Oh, and G. A. Smith, Phys. Rev. Lett. 29, 675 (1972).

⁴³T. Ferbel, Phys. Rev. Lett. 29, 448 (1972).

⁴⁴R. S. Panvini *et al.*, Phys. Lett. 38B, 55 (1972).